ALJEST

Enhance Wear resistance of A2024-T4 Aluminum alloy after Conventional Anodizing

N. Tekkouk[1], M. Arbaoui*, S. Abdi, A. Rezzoug

[1] Faculté des hydrocarbures et de la chimie
Université M'hamed BOUGARA, Boumerdes, 35000 Boumerdes–Algeria

*Corresponding author: n.tekkouk@univ-boumerdes.dz; Tel.: +213 00 00 00; Fax: +21300 00 00

ARTICLE INFO	ABSTRACT/RESUME
	Abstract: Allowing reducing CO2 emission in automotive industry, design engineers gradually replacing steel and grey iron by aluminum alloys due to its low density. The aim of the present paper is to investigate the effect of anodic layer on friction coefficient (COF) and wear resistance of 2024A anodized aluminum alloy by using different techniques of analysis such as Tribometer and Micro-scratch tester. The derived laws from the friction theory shows that as the sliding speed increases are the wear resistance decreases. However, during our experiences, we have observed that this is not true for all increasing speed values. The tests are carried out at different loads conditions and at different sliding speed and hardness, wear rate and COF have been measured after and before anodizing process, metallurgical characterization was assessed using SEM microscope and XRD analysis. *The results show when speed reaches the value of u=0.4m/s the wear mechanism is transformed from the severe regime to mild regime, which is considered as a significant reduction in wear rate and COF at this transition speed.*

I. Introduction

Grey iron has good mechanical properties as: hardness, good wear resistance but it is less resistant to stress and denser than aluminum alloys [1, 2]. Therefore, a pure aluminum has poor mechanical properties that could be enhanced; this has been proven by many studies [3-6]. Melik Çetin [7] has examined the effect of manganese (wt %) and size of the Al_2O_3 abrasive grains on abrasive wear behaviors of Al–Si–(0.16–0.76%) Mn, another interesting work has been done by Priet and al [8] who has studied the effect of new sealing treatments on corrosion fatigue life time of anodized A2024 aluminum alloy, and has confirmed that the A2024 aluminum alloy has good mechanical properties [8], it is fluently used in aeronautic industry, and it is often selected for the excellent adhesion of the protective oxide layer to the substrate, so the anodic film is composed of a compact inner layer and a porous outer layer which can be sealed to improve the

corrosion resistance [8]. Anodization is an electrochemical process for producing an oxide coating (alumina) on the surface of the metal in order to increase its resistance to corrosion [8] and abrasion [9]; electrochemical process is controlled by four factors: acid concentration (C_a), electrolyte temperature (T°), current density (di) and the processing duration (t). A conventional anodizing (C.A) by sulfuric acid is obtained at :di= (1,2-1,5) A/dm^2 , C_a (H_2SO_4)= (180-220)g/l, T°= (20±5)°c , t=(20-30) mn [9, 10], the thickness of the layer obtained by conventional anodizing varies between 10 to 20 µm [9], in the current study we aim to evaluate the Tribology properties of anodic film on the surface of 2024A aluminum alloy under dry and severe wear conditions, The reason behind to use anodic film is used as a surface coating in order to enhance the wear resistance of the alloy, as non protected alloy is subject to fast wear . Wear is quantified by wear rate (k) and the good indicator of wear rate is the friction coefficient (COF) which

is proportional to it. In addition, we investigate the effect of sliding speed on wear rate and COF in order to extract the optimal speed that keeps COF and wear rate in low level.

II. EXPERIMENTAL PROCEDURE

II.1. Description of test device

The experimentales tests are carried out by using a pin-on-disk **CSM** Tribometer (**Fig.1-a**) and the samples used as disk are A2024 aluminum alloys of (35 * 35 * 8) mm³ dimensions and the second used as pin is steel ball of 100Cr6, the latter sliding on the flat face of a sample (Fig.1 (a)), rotating in a horizontal plane with provisions for controlling load, speed, and for measuring friction.

The aluminum alloys are prepared on the contact surface before each test with abrasive paper up to 1200 μm roughness. After that, the arithmetic mean roughness (Ra) is measured by a Tylor Hobson stylus profilometer in each sample. Tests performed by the Micro scratch Tester, the micro scratch test (Figure 1(b)) determine the properties of adhesion, friction, wear resistance and fatigue on materials and thin coating.
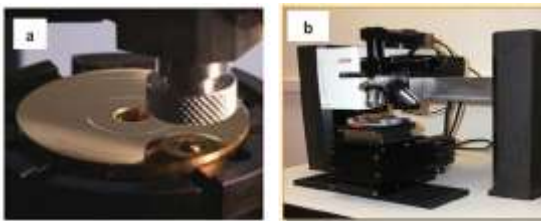

Figure1. *Friction tests: (**a**) CSM Pin-on-disk wear test machine, (**b**) Micro Scratch Tester*

II.2. Test materials

The chemical composition of the alloy is characterized by the device EDX, view table 1. The chemical composition of steel 100Cr6 is mentioned in table 2 according to Ref (11). The mechanical characteristics of the pairs are described in Table 3.

Table 1. *Chemical composition of A2024-T4*

Chemical composition (%)						
Al	Cu	Mg	Si	Fe	Mn	Zn
Rest	4.009	1.753	0.331	0.329	0.238	0.078

Table 2. *Chemical composition of 00Cr6[11]*

Chemical composition (%)					
Fe	C	Si	Mn	Fe	Cr
Reste	1.0	0.25	0.3	0.329	1.5

Table 3. *Mechanical characteristics*

Properties / Materials	Hardness	Module Elasticity (MPa)	Density
100Cr6 [11]	305 HV	210000	7.8
2024A	135 HV	73000	2.78

II.3 Friction alloy properties
II.3.1 Wear tests

The tests carried out before anodizing are represented in table 3.

The coefficient of friction (COF) has been chosen as an evaluation parameter for tribological characteristics because it is the direct expression of the energy expended which dissipates as heat (E_d) as the equation [12]: $E_d=Q.u.f.$

The figure 2 presents the COF values of substrate under test condition mentioned in table 4. The figure 2 show that the COF values of the alloy before anodizing is never stable because at small sliding distances COF marks a sudden rise to 0.6 after that it go up to 0.9, so there is a bad friction behavior because the value of COF is high, at most the sliding distance is very small because the Tribometer machine is programmed to stop at f=1 to avoid vibration due to the seizure phenomenon.

Table 4. *Tests conditions*

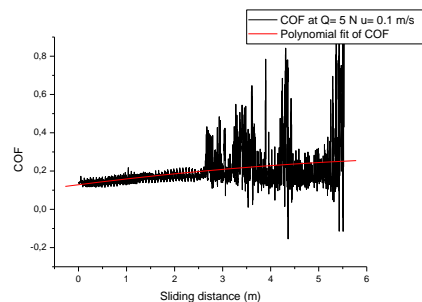| Type	Sample	Ra (μm)	Load (N)	Sliding speed (m/s)	Sliding distance (m)
dry	7,8	0.22	5	0.1	100,250

Figure2. *friction coefficient (f) in dry conditions at: Q= 5N, u=0.1 m/s*

II.3.2 Micro-scratch tests

The principle of the scratch test (Micro Scratch Tester) is to push an indenting diamond hard point in a straight line at different progressives increasing loads. This device is equipped with an optical microscope, mounted in a system that can measure COF and depth of indenter penetration as well as residual depth; the results are showed in figure 3.The micro scratch tester achieves scratches from 0.03 to 5 N at a low speed u = 0.16 mm / s at a distance of d = 4mm, we note that the COF is in linear progression from f = 0.10 to f = 0.4 (Fig. 3 (a)). So, when the load achieve Q = 5 N the value of COF is f=0.4 at constant speed and the penetration depth reaches 7µm (fig.3 (b)).

The fig.3 presents the result of the micro-scratch test: COF at Q = 5N is remarkable (f = 0.4) is very smaller than that in the results of Tribometre (Fig.2) when Q = 5 N (f_{mean} = 0.8) because the speed conducted by scratch-test machine is very smaller than that done by wear tests machine (u = 0.16 mm/s <<< u = 100 mm/s`), so the increase in the sliding speed generates a lot of heat in the surface of contact which causes welding of the sample on the pin, and causes a sliding phenomenon.
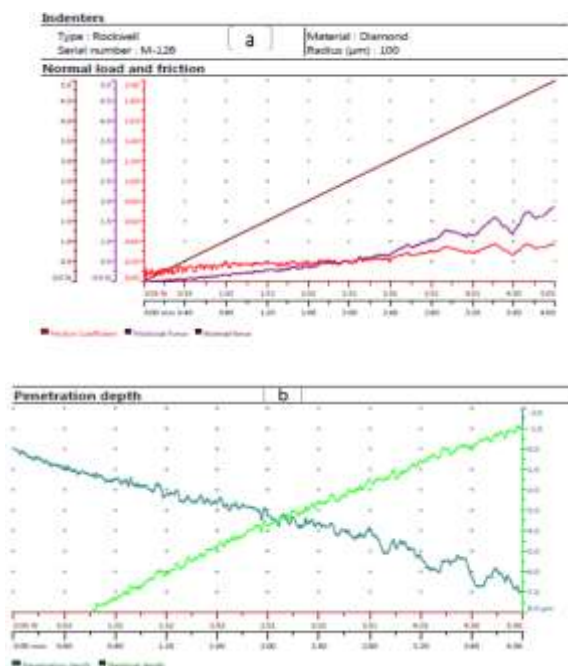

*Figure 3. Scratch Test Results of alloy substrate up to 5N: **a:** COF values **b:** depth of indenter penetration*

III. Anodizing

III.1 Conventional Anodizing processes

After sanded and cleaned of the samples with acetone, anodizing was carried out in the laboratory with sulfuric acid which had 180 g/l acid concentration, view fig. 4(a), at (20 ± 5) °c used lead cathode and the aluminum alloy as the anode. All specimens were anodized at constant voltage U = 12 V for t = 25 mn and di = 1.5 A/dm². After anodizing, specimens were washed in distilled water and after that they were sealed with drilling distilled water.

The figure 4(a) shows the anodizing process device in laboratory, the figure 4(b) present the sealing step.

The SEM images were obtained by electronic microscope QUANTA 650, the figure.5(a) present the thickness of anodic layer, the figure 5(b) show the morphology of anodic layer, this last presents some pores; the majority of pores are filled in a sealing step. The layer has about 11, 81 µm thicknesses (Fig. 5(a)).

The characterization of the anodic coating by XRD analysis is showed in figure 6.

The indexation of the diffraction peaks was made using the ASTM sheet of the aluminum (Al) and the peaks of alumina (αAl_2O_3) [13, 14], the figure 6 displays four peaks of αAl_2O_3 which represent the anodic oxide coating of the alloy.

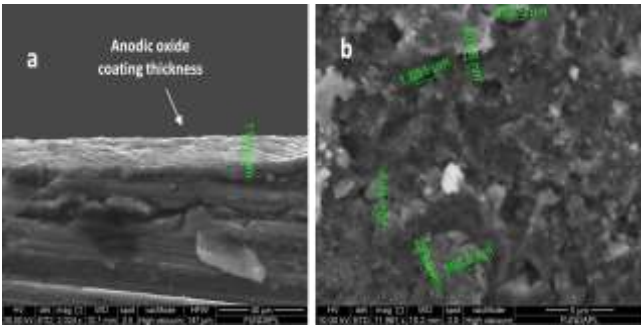*Figure 4. Anodizing processes: (**a**) Device, (**b**)*

Sealing step.

Figure 5. *SEM images: (a) Oxide layer thickness, (b) Anodic layer morphology*

Figur 7. *Friction coefficient (f) in dry conditions : (a) Before anodizing, (b) After anodizing*
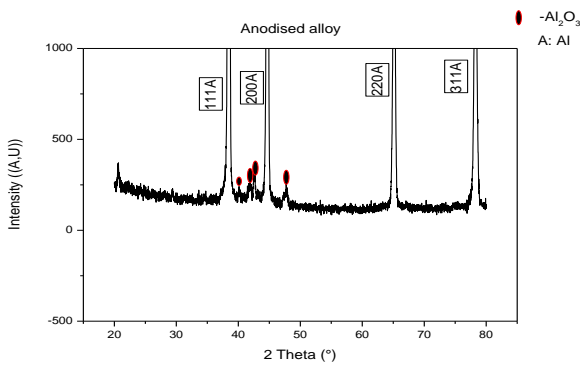

Figure 6. *XRD results of the alloy covered by anodic layer*

III.2 Friction properties

III.2.1 Tribometer tests

The table 5 present the test conditions applied on alloy after anodizing in wear tests with an alloy before anodizing at the same speed u = 0.5m/s.

The figure 7(a) show that COF values are never stable and marks various fluctuation because at small sliding distance it reach a high value f = 1 and Tribometer is stopped.

COF values in the second figure 7(b) are stable and mark a good mean value f=0.45 compared with the first figure, because the surface of alloy become well hard, the hardness values are mentioned in table 6. We can compare this value after anodizing for that of grey cast iron [1].

Table 5. *Tests conditions*

III.2.2 Micro-scratch tests

Figures 8 show the results of scratches obtained under the last same operating conditions applied now on alloy coated by conventional anodizing.

COF in figure 8 (a) is in linear progression from f = 0.03 to f = 0.3, we note a significant amelioration in COF values compared with that of substrate before anodizing (figure 3) and at the end of test when Q = 5N the COF has the value f = 0.3 < f= 0.4 in figure 3. The friction properties are enhanced due to the oxide coating added after anodizing. The results of COF: f = 0.3 indicate that the indenter doesn't reach the substrate, and the depth penetration is about 8µm (fig.8 (b)). The COF value at 5 N during wear tests (Fig. 7 (b)) f = 0.45 > f = 0.3 obtained by using the micro scratch test because the sliding speed done from scratch-tester is lower than that done by wear test machine (u = 0.16 mm/s < 500 mm/s).

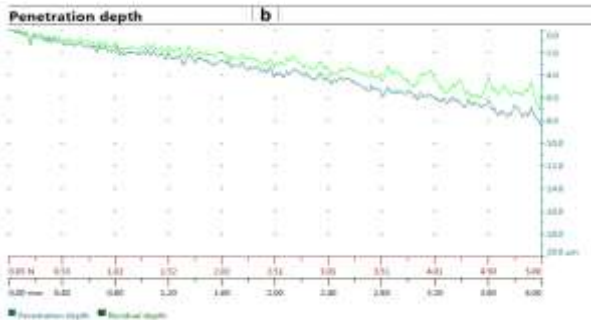|	Sample	Ra (µm)	Load (N)	Sliding speed (m/s)	Time (mn)
Dry	11,12	0.22	5	0.5	16
Dry	9,10	0.43	5	0.5	16
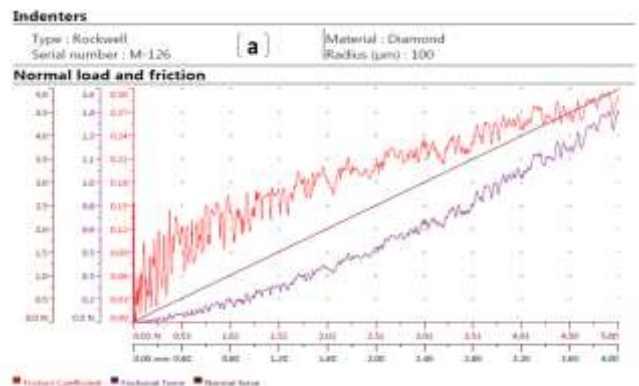
Figure 8. Scratch Test Results of anodizing alloy up to 5 N: (a) COF values, (b) depth of indenter penetration

Table 6. Hardness results

Al-Cu-Mg alloy samples		Micro Hardness
Before anodizing	Ra= 0.22μm	H=135 HV
After anodizing	Ra= 0.43	238 HV
Grey iron G3500	/	H=207-255 HV

III.3.2 Calculate of wear rate (K)

The wear rate values were calculated by the equation [15]: $K= \frac{\Delta V}{Q.L}$ where ΔV is the wear volume loss, Q is the normal load and L is the sliding distance.

The **table 7** gives the results of wear rate and COF values at different load charge and sliding speed and the wear rate values are modeled in figure 9.
speed (u) increase the energy (E_d) increase and COF increase too, but at 10N is not the case because when **u** increase exactly between (0.3 to 0.5 m/s), **COF** decrease and **E_d** increase sensibly, so COF is not always the direct expression of E_d. But the results of wear rate (figure 9) and COF (figure 10) are significant; when **COF** increase **K** increase and when **COF** decrease **K** decrease too but the relationship between **COF** and **K** is independent because when the values of COF is the same or approximately the same; the values of **K** are different; for example in Table 6 when u = 0.3m/s at Q = 10N   K = 0.0134 mm³/N.m and **f = 0.44** and at Q = 5N at u = 0.3 m/s   K = 0.0047mm³/N.m even so **f** = 0.44. The value of k when u = 0.4m/s is K = 0.0003mm³/N.m is the best

value for the all tests, so the alloy is sensibly worn and according to ref (16) the wear regime is **mild** so it was a transition from severe wear to mild wear [16] at u = 0.4m/s when Q = 10N, and the figure 11 presents the COF profile when u = 0.4m/s compared for that when u = 0.3m/s.

In the objectives to calculate the wear volume, the samples are weighed before and after each wear tests using CRYSTAL microbalance to within ± 10⁻⁴ g accuracy.
The COF values are modeled in figure 10.
At 5N load charge the results of figure 10 confirm the equation: $E_d = Q.u.f$, that the friction coefficient is the direct expression of the energy expended which dissipates as heat because when sliding.
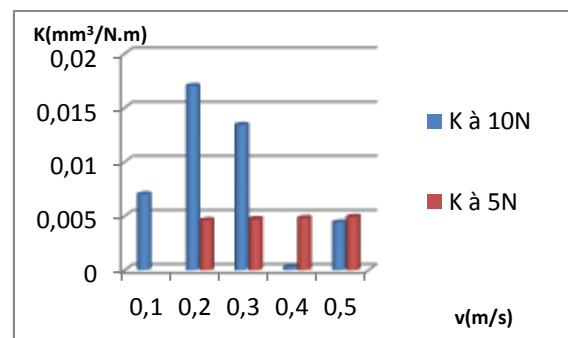

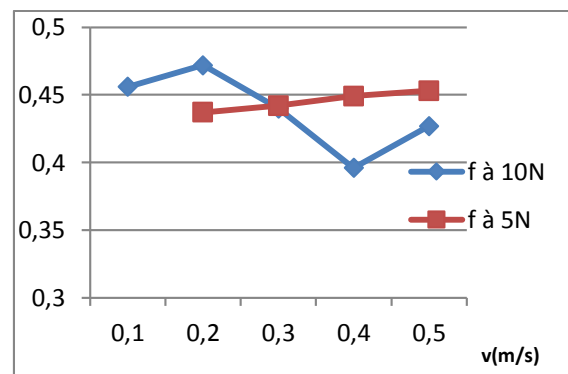*Figure 9. Wear rates of anodized samples at different sliding speed*

Figure 10. COF of Anodized samples at different sliding speed

Table 7. Wear rate of anodized samples

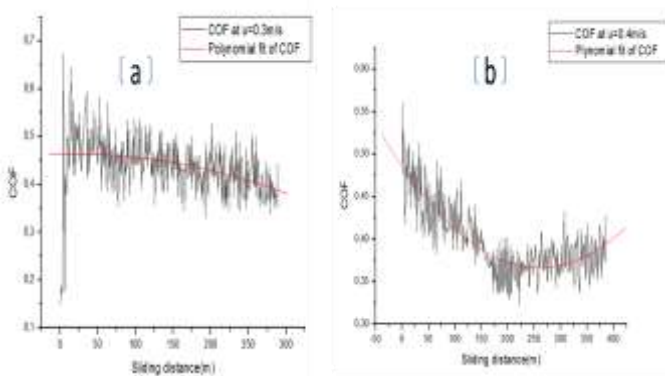| N°	Ra	Q (N)	u (m/s)	L(m)	ΔV (mm^3)	K (mm^3/N.m)	f average
13	0.43	10	0,1	395	27,800	**0,0070**	**0,456**
14	0.43	10	0,2	200	34,632	**0,0170**	**0,472**
15	0.43	10	0,3	288	38,086	**0,0134**	**0,440**
16	0.43	10	0,4	384	01,151	**0,0003**	**0,396**
10	0.43	10	0,5	500	22,796	**0,0044**	**0,427**
17	0.43	5	0,2	200	4,448	**0,0046**	**0,437**
18	0.43	5	0,3	300	7,05	**0,0047**	**0,442**
19	0.43	5	0,4	400	9,6	**0,0048**	**0,449**
20	0.43	5	0,5	503	12,510	**0,0049**	**0,453**

Figure 11. *COF at* **Q** *= 10N: (**a**) u = 0.3m/s, (**b**) u = 0.4 m/s*

III.3.3 Wear behavior

The first apparent remark in figure 12(a), is the width (W) of the wear trace; the trace when u = 0.4m/s is smaller than their when u = 0.3m/s (W (P_2) <W (P_1)), which indicate that the wear volume loss decrease in P_2.

The surface apparent of alloy in P_1 is greater than in P_2, the number of cracks in figure 12(b) is more than in figure 12(c), that confirm which the wear volume loss affected at 0.4m/s become lower than it in figure 12(b) when u = 0.3m/s, so how explain this phenomenon. The explanation is when the sliding speed increase, it affect dissipative of structures form by kinetic phase transition occurring under the cooperative (synergetic) actions of strain, mass transfer and heating [17], which result the increasing in hardness which affects transition from severe wear to mild wear of the anodized alloy.

The figure 13 presents the sequences of wear behavior of the oxide coating surface.

At the figure 13 the different consequences of abrasive wear resulting from degrees of shock exerted by the peers, we start with increasing order of degrees of deformation, and we have:

Cracks is the beginning of plastic deformation, they are small holes wider and deeper than grooves, they are clearly visible in Figure 13(a) and the crack begins to widen and enlarge because of the cumulative shocks exerted by the peers, and a crack propagates and became several cracks see in Figure 13(a) too.

Tearing of layer Due to the cyclic stresses exerted by the pairs, the thickness of the oxide layer will decrease and the cracks will disappear and they become scattered oxide debris everywhere in the surface of alloy (figure 13(b)).

Perforation in the end, the oxide layer is totally deteriorated and the substrate of alloy is clearly visible in figure 13(c) at the edge of the wear trace.

III.3.3 Wear behavior

The first apparent remark in figure 12(a), is the width (W) mentioned in table 8 of the trace when u = 0.4m/s is smaller than they're when u = 0.3m/s (W (P_2) <W (P_1)), which indicate that the wear volume loss decrease in P_2.

The surface apparent of alloy in P_1 is greater than in P_2, the number of cracks in figure 12(b) is more than in figure 12(c), that confirm which the wear volume loss affected at 0.4m/s becomes lower than it in figure 12(b) when u = 0.3m/s, so how explain this phenomenon. The explanation is when the sliding speed increase, it affect dissipative of structures form by kinetic phase transition occurring under the cooperative (synergetic) actions of strain, mass transfer and heating [17], which result the increasing in hardness which affects transition from severe wear to mild wear of the anodized alloy.

The figure 13 presents the sequences of wear behavior of the oxide coating surface.

At the figure 13 the different consequences of abrasive wear resulting from degrees of shock exerted by the peers, we start with increasing order of degrees of deformation, and we have:

Cracks is the beginning of plastic deformation, they are small holes wider and deeper than grooves, they are clearly visible in Figure 13(a) and the crack begins to widen and enlarge because of the cumulative shocks exerted by the peers, and a crack

propagates and became several cracks see in Figure 13(a) too.

Tearing of layer Due to the cyclic stresses exerted by the pairs, the thickness of the oxide layer will decrease and the cracks will disappear and they become scattered oxide debris everywhere in the surface of alloy (figure 13(b)).

Perforation in the end, the oxide layer is totally deteriorated and the substrate of alloy is clearly visible in figure 13(c) at the edge of the wear trace.
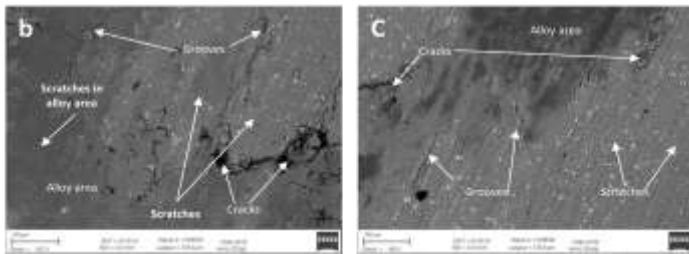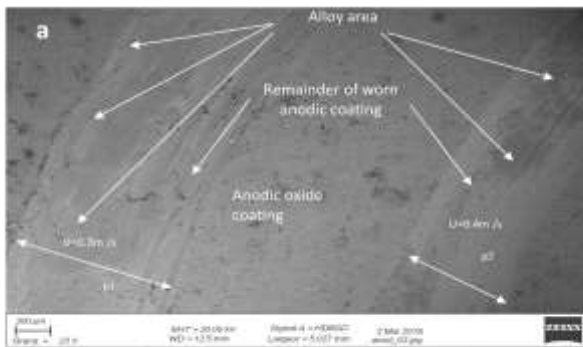

Figure 12. *SEM image of worn oxide coating traces **b**: u = 0.3m/s, **C**: u = 0.4m/s*
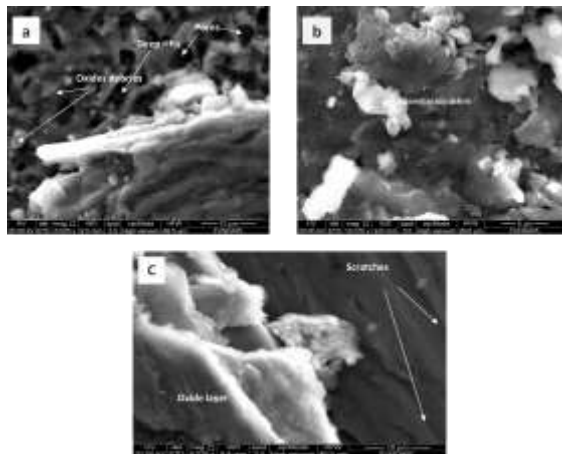
Figure 13. *Wear behavior of oxide coating surface*

Table 8. Nomenclature

Symboles	Nomenclature	Unit
E_d	Energy dissipated	J
Q	Normal load transmitted	N
f	Friction Coefficient	/
u	Sliding velocity	m/s
E	Young's module	GPa
L	Sliding distance	m
H	Hardness Vickers (HV)	MPa
d	Density	g/cm^3
Ra	Arithmetic mean roughness	μm
di	Current density	A/dm^2
w	Wide trace	μm

IV. Conclusion

At low sliding speeds the alloy gives good friction properties, and when the speeds increases the COF increase and wear rate increase too. But at an increasing sliding speed the wear rate decrease the wear mechanism affect transition from severe wear to mild wear, the value of transition in previous tests is u = 0,4 m/s. At this sliding speed, the contact surface has an improvement of the characteristics, that is to say, it becomes harder under the cooperative (synergistic) actions of deformation, mass transfer and heating and improves the properties resistance to wear and friction in the contact surface of the alloy. The friction coefficient is the direct expression of the wear rate of the alloy, but they are independent. The 2024A-T4 aluminum alloy provides a good friction and hardness properties when the alloy is covers with a regular anodic oxide coating.

V. References

1. Terheci, M.; Manory, R..; Herde, J. The friction and wear of automotive grey cast iron under dry sliding conditions part 1- relationships between wear loss and testing- parameters. *Wear*180 (1995) 73-78.
2. Hana, J.; Zhanga, R.; Ajayib, O.; Barbera, G.; Zoua, Q.; Guessousa, L.; Schalla, D.; Alnabulsic, S. Scuffing behavior of gray iron and 1080 steel in reciprocating and rotational Sliding. *Wear*271(2011) 1854- 1861.
3. Mina, M.; Bastwros, H.; Amal, M.; Esawi, K.; Abdalla, Wi.Friction and wear behavior of Al-CNT composites. *Wear*307 (2013) 164-173.
4. Devaraju, A.; Kumar, A.; Kumaras, A.; Kotiveerachari, B. Influence of

reinforcements(SiCandAl₂O₃) and rotational speed on wear and mechanical properties of aluminum alloy 6061-T6 based surface hybrid composites produced via frictions tir processing. *Materials and Design*51(2013) 331-341.

5. Chen, F.; Wang, F.; Zong-ning, C.; Feng, M.; Qiang, H.; Zhi-qiang, C. Microstructure mechanical properties and wear behaviour of Zn_2in situ composites. *Trans. Nonferrous Met. Soc. China*25 (2015) 103.

6. Duradji, V.; Kaputkin, D.; Duradj, i. Aluminium Treatment in the Electrolytic Plasma During the Anodic Process. *JOURNAL OF Engineering Science and Technology Review*10 (3) (2017) 81-84.

7. Melik, Ç. Abrasive wear behaviour of cast Al-Si-Mn alloys Proceedings of the Institution of Mechanical Engineers, Part E. *Journal of Process Mechanical Engineering*233(4) (2018) 908-918.

8. Priet, B.; Grégory, O.; Christine, B.; Kévin, G.; Laurent, A. Effect of new sealing treatments on corrosion fatigue life time of anodized 2024 aluminium alloy. *Surface & Coatings Technology*307 (2016) 206-219.

9. Lebik, H. ; Ait-Amar, R. ; Elhadi, F. ; Madjene, D. Anodic oxidation of methylene blue at Ti/Pt electrode**.** *Algerian Journal of Environmental Science and Technology* (2019) 5 N°3.

10. Gilbert, F. Influence des conditions d'anodisation dure de l'aluminium (AA6061-T6) sur la couche d'oxyde formée. faculté des sciences et génie université laval Québec: Mémoire pour l'obtention du grade de Maître es sciences (M.Sc.) (2011) p. 6 :12.

11. M, Arbaoui. Étude phénoménologique des surfaces antagonistes (palier lisse) dans les processus d'abrasion lubrifié. université MOULOUD MAMMERI- TIZI-OUZOU (2008).

12. Cartier, M.; Kapsa, P.Usure des contacts mécanique, Problématique et définitions. *Technique de l'ingénieur*BM 5065 (2012) p 6.

13. Fares, C.; Hemmouche, L.; Belouchrani, M.A.; Amrouche, A.; Chicot, D.; Puchi-Cabrera, E.S. Coupled effects of substrate microstructure and sulphuric acid anodizing on fatigue life of 2017A aluminum alloy. *Materials and Design*86 (2015)723-734.

14. JCPDS ICDD, carte N°04-0787(1997).

15. Andrade, T.F.; Wiebeck, H.; Sinatora, A. Effect of surface finishing on friction and wear of Poly-Ether-Ether-Ketone (PEEK) under oil lubrication. *Polímeros*26 (2016) 336-342.

16. Tekkouk, N.; Arbaoui, M.; Abdi, S.; Rezzoug, A.TRANSITION BETWEEN SEVERE AND MILD WEAR of 2024A-T4 Anodized Aluminum Alloy under Severe Wear Conditions. *Journal of t he Koren Physical Society*76 (2020) 899-903.

17. Kostetsky, B.I.The structural-energetic concept in the theory of friction and wear synergism and self organization. *Wear*159 (1992) 1-15.

Please cite this Article as:
Tekkouk N., Arbaoui M., Abdi S., Rezzoug A., Enhance Wear resistance of A2024-T4 Aluminum alloy after Conventional Anodizing, ***Algerian J. Env. Sc. Technology**, **7:2 (2021) 1841-1848***